One-Pot Synthesis of Core−Shell FeRh Nanoparticles

Diana Ciuculescu,[†] Catherine Amiens,*[,†] Marc Respaud,[‡] Andrea Falqui,[‡] Pierre Lecante,[§] Robert E. Benfield,[||] Linqin Jiang,[⊥] Kai Fauth,[⊥] and Bruno Chaudret[†]

Laboratoire de Chimie de Coordination, UPR 8241-CNRS, 205 Route de Narbonne, F-31077 Toulouse, France, Laboratoire de Physique et Chimie des Nano-Objets, INSA, 135 Avenue de Rangueil, F-31077 Toulouse, France, Centre d'Elaboration des Matériaux et d'Etudes Structurales, CNRS, 29 Rue Jeanne Marvig, BP 4347, F-31055 Toulouse, France, Functional Materials Group, School of Physical Sciences, University of Kent, Canterbury CT2 7NH, U.K., and Max-Planck-Institut für Metallforschung, Heisenbergstrasse 3, D-70569 Stuttgart, Germany

Received June 8, 2007
Revised Manuscript Received July 27, 2007

Depending on the chemical composition and ordering of the system, alloying of a 4d element displaying a large magnetic susceptibility with a 3d ferromagnetic one induces a polarization of the 4d element and a strong enhancement of the overall magnetization. Furthermore, certain 4d elements, among them Rh, become ferromagnetic below a critical size.[1] As a consequence of the induced polarization and large spin orbit coupling in the 4d elements, the magnetocrystalline anisotropy is also affected. We took advantage of these effects, in the case of the CoRh system, and demonstrated that combining such a 3d/4d association and size reduction leads to CoRh nanoparticles (NPs) of outstanding magnetic properties.[2,3] Surprisingly, these CoRh NPs show partial segregation of the metals, that is, display a core enriched in Rh atoms while their surface is enriched in Co atoms.[4] We next decided to study the FeRh system at the nanoscale, with the objective of synthesizing core(Rh)−shell-(Fe) Rh@Fe NPs. This system is interesting because the FeRh structural and magnetic phase diagrams are particularly rich in the bulk.[5] Also, Fe magnetism is strongly sensitive both to structural properties (metal−metal distance and crystalline structure) and chemical environment.[6] Recently a renewed interest in this system has stimulated much research in the area of Fe−Rh multilayer composites,[7,8] which could serve as a good starting point for understanding the properties of core−shell Rh@Fe NPs. For such small systems, the high surface to volume ratio induces a high reactivity, especially toward any adventitious dioxygen. It is thus of prime importance to reduce the number of synthesis steps. We have now designed a one-pot synthesis based on the hydrogenation of metal−organic complexes. $Rh(allyl)_3$[9] and $Fe[N(SiMe_3)_2]_2$[10] have been selected as metal precursors. Indeed, hydrogenation of $Rh(allyl)_3$ generates only propane as a byproduct and is characterized by very fast kinetics, in contrast to, for example, the Rh(COD)(acac) complex which was used for the synthesis of CoRh NPs.[2] $Fe[N(SiMe_3)_2]_2$ was successfully used for the production of pure Fe NPs.[11,12] These particles displayed enhanced magnetic moments in quantitative agreement with measurements on bare gas-phase particles,[13] demonstrating that hexamethyldisilazane, produced in the hydrogenation step, is innocuous regarding one of the most sensitive physical parameters of the material. This step is slow, however, and requires thermal activation. Hence, exposure of a mixture of both precursors to H_2 should lead first to the formation of Rh NPs. These Rh NPs would then serve as seeds for the growth of the Fe over-layer and produce NPs which could be suitable for fundamental physics studies. To secure a segregated system with a small Rh core, we focused on the $Rh_{20}Fe_{80}$ composition. The presence of a long chain ligand is mandatory during the synthesis to control the final spacing of the NPs. Hexadecylamine (HDA) has previously been used to stabilize Rh NPs.[14] It was demonstrated to be a very labile ligand[15] and so would not prevent the formation of an Fe over-layer on the Rh seeds and would not alter the magnetic properties of surface atoms.[16] We report in this communication the success of this first one-pot synthesis of Rh@Fe NPs and the first results from the study of their structural and magnetic properties. Extreme care was taken to ensure that postsynthesis oxidation did not occur.

Figure 1 shows the final NPs as observed by TEM. From a Gaussian fit, the NPs have a mean diameter of 2.1 nm (standard deviation, $\sigma = 0.6$ nm; Supporting Information). Repeated energy dispersive X-ray (EDX) analyses show the presence of isolated NPs containing both metals (Supporting Information). Their structure was investigated by wide-angle X-ray scattering (WAXS) measurements. In Figure 1, the

[†] LCC-UPR 8241-CNRS.
[‡] INSA.
[§] CEMES-UPR 8011-CNRS.
[||] University of Kent.
[⊥] Max-Planck-Institut für Metallforschung.

(1) Cox, A. J.; Louderback, J. G.; Apsel, S. E.; Bloomfield, L. A. *Phys. Rev. B* **1994**, *49*, 12295.
(2) Zitoun, D.; Respaud, M.; Amiens, C.; Chaudret, B.; Serres, A.; Casanove, M.-J.; Fromen, M.-C.; Lecante, P. *Phys. Rev. Lett.* **2002**, *89*, 37203.
(3) Munoz-Navia, M.; Dorantes-Dávila, J.; Zitoun, D.; Amiens, C.; Chaudret, B.; Casanove, M.-J.; Lecante, P.; Jaouen, N.; Rogalev, A.; Respaud, M.; Pastor, G. M. *Faraday Discuss.* **2007**, in press.
(4) Fromen, M.-C.; Lecante, P.; Casanove, M.-J.; Guillemaud, P. B.; Zitoun, D.; Amiens, C.; Chaudret, B.; Respaud, M.; Benfield, R. E. *Phys. Rev. B* **2004**, *69*, 235416.
(5) Shirane, G.; Chen, C. W.; Flinn, P. A.; Nathans, R. *Phys. Rev.* **1963**, *131*, 183.
(6) Paduani, C.; da Silva, E. G. *J. Magn. Magn. Mater.* **1994**, *134*, 161.
(7) Busch, M.; Gruyters, M.; Winter, H. *Surf. Sci.* **2005**, *582*, 31.
(8) Hayashi, K.; Sawada, M.; Yamagami, H.; Kimura, A.; Kakizaki, A. *J. Phys. Soc. Jpn.* **2004**, *73*, 2550.
(9) Beckhaus, R. Alkenyl, Allyl, and Dienyl Complexes of Main Group Elements and Transition Metals. In *Synthetic Methods of Organometallic and Inorganic Chemistry*; Herrmann, W. A., Ed.; Georg Thieme, Verlag Stuttgart: New York, 2000; Vol. 9, p 38.
(10) Andersen, R. A.; Faegri, K.; Green, J. C.; Haaland, A.; Lappert, Leung, M. F., W.-P.; Rypdal, K. *Inorg. Chem.* **1988**, *27*, 1782.
(11) Dumestre, F.; Chaudret, B.; Amiens, C.; Renaud, P.; Fejes, P. *Science* **2004**, *303*, 821.
(12) Margeat, O.; Respaud, M.; Amiens, C.; Lecante, P.; Chaudret, B. *Phys. Rev. B*, submitted.
(13) Billas, I. M.; Chatelain, A.; Heer, W. A. D. *Science* **1994**, *265*, 1682.
(14) Ramirez-Meneses, E. Synthesis and characterisation of Rh, Pt and Pd metal NPs, stabilised by ligands. Ph.D. dissertation, Université Paul-Sabatier, Toulouse, 2004.
(15) Pan, C.; Pelzer, K.; Philippot, K.; Chaudret, B.; Dassenoy, F.; Lecante, P.; Casanove, M. J. *J. Am. Chem. Soc.* **2001**, *123*, 7584.
(16) Cordente, N.; Amiens, C.; Chaudret, B.; Respaud, M.; Senocq, F.; Casanove, M.-J. *J. Appl. Phys.* **2003**, *94*, 6358.

10.1021/cm0715343 CCC: $37.00
Published on Web 08/18/2007

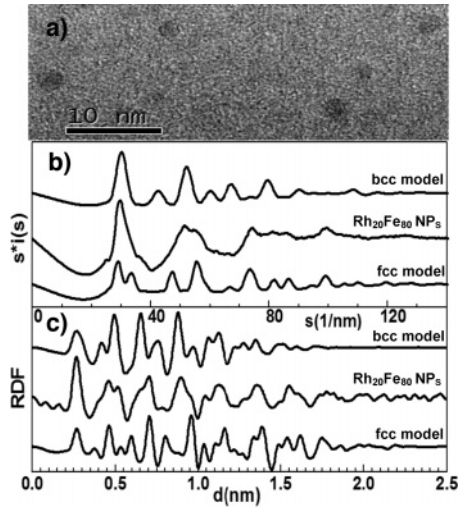

Figure 1. (a) TEM image of $Rh_{20}Fe_{80}$ NPs. Experimental data obtained from WAXS measurements and compared to computed curves from bcc Fe and fcc Rh model clusters: (b) reciprocal space, (c) direct space.

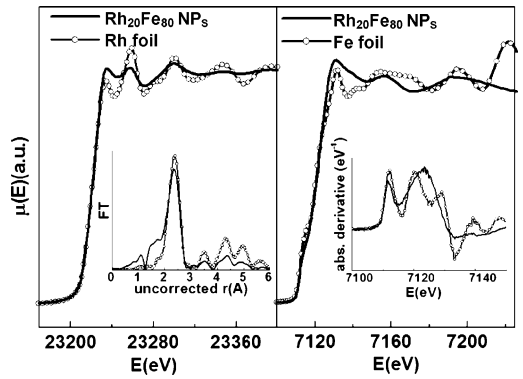

Figure 2. Left: XAS at Rh K-edge (inset: uncorrected RDF). Right: Fe K-edge (inset: first derivative in XANES region).

experimental reduced intensity and corresponding radial distribution function (RDF) of $Rh_{20}Fe_{80}$ NP_S are compared to those computed from two model structures, consisting of bcc (α-iron like) and fcc (rhodium and γ-iron like) clusters, respectively. Comparison, both in direct and in reciprocal space, shows that the $Rh_{20}Fe_{80}$ samples do not crystallize in a bcc arrangement. They thus possess a different atomic packing than in the thermodynamically stable bulk alloy of the same composition, which is of bcc type.[5] In particular, the experimental data in reciprocal space do not display the peak at 45 nm^{-1} which is typical of the bcc structure. The RDF of the bcc model displays a broader peak for the first metal−metal distance, and the relative intensities of the next two peaks are changed. The RDF and reduced intensity are closer to those calculated from the fcc model cluster. The metal bond length, 0.265 nm, is larger than in bulk Fe (0.248 nm) and bulk $Rh_{20}Fe_{80}$ alloy (0.253 nm) but is closer to that of bulk Rh (0.269 nm). This is typical for clustering of Rh atoms, that is, formation of segregated NPs.[4] X-ray absorption spectroscopy (XAS) was further used to investigate each metal separately (Figure 2, Supporting Information).

In Figure 2, the Rh K-edge is very similar to that measured on a Rh foil, indicating that oxidation was successfully prevented. The EXAFS oscillations are damped (as a result of finite NP size) but in phase with those of the bulk reference. The fourier transform (inset, Figure 2) shows a metal bond

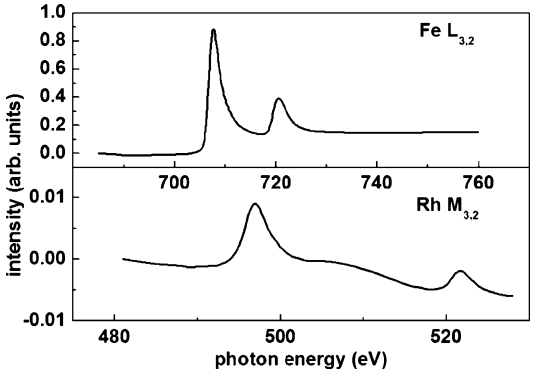

Figure 3. XAS measurements at (top) Fe $L_{3,2}$ and (bottom) Rh $M_{3,2}$-edges.

length identical to that in the reference Rh foil. All these observations point to Rh clustering in the NPs. Poorer data quality prevents complete treatment at the Fe K-edge. Still, the line shape of the Fe K-edge is appreciably different from that of the bcc Fe reference but is typical of unoxidized metallic iron (inset, Figure 2) with an amorphous packing.[17] The shapes of the $L_{3,2}$ and $M_{3,2}$ edges, studied during X-ray magnetic circular dichroism (XMCD) measurements (see below), give further clear evidence for the absence of oxide contamination (Figure 3). The results obtained from the analysis of both WAXS and XAS strongly support the presence of segregated NPs. Morphological and structural evolution as a function of the reaction time were studied by transmission electron microscopy (TEM) and WAXS (Supporting Information). After 1 h, TEM images display small NPs, some of which are agglomerated. EDX analysis on these NPs shows mainly the presence of Rh, while the diffuse background contains mainly Fe (Supporting Information). For longer reaction times, the morphology of the NPs does not change much, but fewer agglomerates are observed. Because of the inherent uncertainty of size determination, conclusive indications on the growth of the NPs could not be derived from size histograms. After 1 h, WAXS measurements show a structural arrangement and a metal bond length identical to that measured for pure Rh NPs, confirming the preferential decomposition of the Rh precursor during the first stage of the reaction. Surprisingly, the general structural features observed for the final $Rh_{20}Fe_{80}$ NPs are already observed after 4 h of reaction. No further structural change could be observed for the sample quenched at 12 h. This could reflect the growth of an amorphous Fe layer. Magnetic properties were not studied as a function of reaction time, because some non-decomposed Fe precursor still remains in the samples at intermediate reaction times. Its magnetic contribution would prevent any conclusive interpretation of the data.

Investigation of the magnetic properties of the final $Rh_{20}Fe_{80}$ NPs was carried out by SQUID (Figure 4). The zero field cooled/field cooled magnetization curve measured at 1 mT is characteristic of a superparamagnetic behavior and displays a very low blocking temperature $T_B = 3$ K. Magnetization loops [$M(H)$] were recorded at 2 K (inset, Figure 4). As expected, the curve provides evidence of

(17) Long, G. J.; Hautot, D.; Pankhurst, Q. A.; Vandormael, D.; Grandjean, F.; Gaspard, J. P.; Briois, V.; Hyeon, T.; Suslick, K. S. *Phys. Rev. B* **1998**, *57*, 10716.

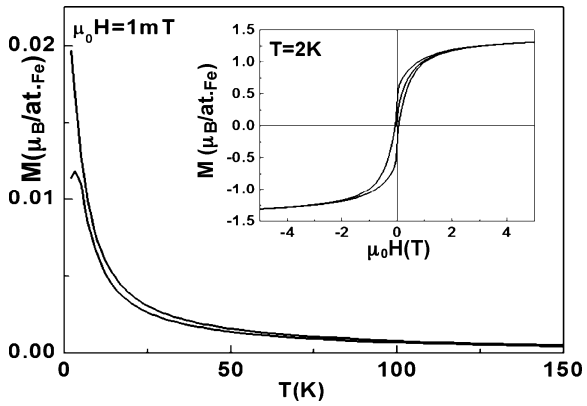

Figure 4. Zero field cooled/field cooled data (inset: hysteresis curve).

hysteresis. At 5 T, the magnetization does not saturate and still displays a large high field differential susceptibility. This is indicative of a non-collinear spin structure. The value of the spontaneous magnetization at 5 T corresponds to an average of 1.3 μ_B per Fe atom, assuming that Rh atoms carry negligible magnetic moments, if any. This value is very small in comparison to $Rh_{20}Fe_{80}$ bulk alloys (>2.9 μ_B)[5] and to bulk or nanosize Fe (2−2.5 μ_B)[18] but very large in comparison to what is observed for thin Fe layers deposited on Rh substrates, where the first two Fe layers are not ferromagnetic.[8,19] XMCD measurements were carried out at both Fe and Rh edges. The dichroic signal measured at Fe $L_{3,2}$ edge is in agreement with the reduced magnetization of Fe in the NPs found by SQUID magnetometry (not shown). At the Rh $M_{3,2}$ edge a much smaller yet finite XMCD signal is observed, indicative of an induced moment with a component parallel to that of Fe. The Rh atoms in $Rh_{20}Fe_{80}$ NPs thus acquire some magnetic polarization, similar to what was observed for the CoRh system. Full interpretation of the data is out of the scope of this paper and will be reported elsewhere.[20]

The kinetic study of the synthesis as well as WAXS and XAS measurements on the final $Rh_{20}Fe_{80}$ system are in agreement with the conclusion that this one-pot synthesis route does indeed yield core−shell NPs. Oxidation was entirely avoided in all experiments, ruling out oxidation as a possible factor inducing chemical segregation in this system, in contrast to what was observed by Gatte and Phillips[21] The better coordination of HDA to Fe surfaces compared to those of Rh might well account for the disappearance of agglomerates at long reaction times. We thus assume that the particles consist of a very small core of Rh atoms, on which Fe tends to grow in a disordered way. The most frequent diameter observed (2 nm) corresponds to NPs with 300−400 atoms in average, 60−80 Rh atoms (20%), and 240−320 Fe ones (80%). When the fact that all Rh atoms are buried in the core of the NPs is considered, they should represent an fcc seed of slightly more than two layers on which two layers of Fe atoms would grow. As the Rh seed is most probably not a close-shell cluster, a mixed Rh−Fe interface probably develops during the growth of the Fe over-layer leading to chemical defects at the interface.

The magnetic properties of this system are striking. Indeed, the first two layers of Fe grown on paramagnetic Rh(100) or (001) surfaces do not display ferromagnetism,[8,19] and density functional theory calculations suggest that this is related to the formation of tetragonally distorted Fe layers upon epitaxial growth on Rh.[22] In our case, the NPs are ferromagnetic. Because Fe magnetism is strongly governed by the interatomic distances and local structure, a first explanation could be that the defects present in the structure of the outer Fe shell of the NPs enable the emergence of ferromagnetism. Local magnetism in bimetallic NPs is far from simple, reflecting the complex interplay of structural and chemical order, finite size effects, and electronic properties,[23] so a better understanding of this system will require theoretical calculations, as done for the 50/50 composition.[24]

In conclusion, we have successfully synthesized core−shell Rh@Fe NPs by a one-pot method taking advantage of the different kinetics of hydrogenation of organometallic precursors, respectively $Rh(allyl)_3$ and $Fe[N(Si(CH_3)_3)_2]_2$. The NPs can be viewed as a curved interface between an fcc Rh core and amorphous Fe overlayers. They display a nonsaturated ferromagnetic character with a spontaneous magnetization far below the bulk one. This reflects the complex magnetism of this core−shell system. As amido complexes are known for many elements, our one-pot synthetic procedure should be general to access core−shell magnetic NPs. The next challenges will be the understanding of the magnetism of this striking system and the development of new strategies to reverse the kinetics of decomposition of amido and alkyl complexes, to get magnetic seeds in noble metal shells.

Acknowledgment. This work was supported by the EC project "Syntorbmag" MCA-RTN 2004-005567, the EC - RIA under the FP6 "Structuring the European Research Area" program (through the Integrated Infrastructure Initiative "Integrating Activity on Synchrotron and Free Electron Laser Science", Contract No. RII 3-CT-2004-506008), at DESY for EXAFS and BESSY for XMCD measurements. We thank Greg Ballentine and Benedikt Friess for assistance during data gathering at BESSY and Alain Mari for recording SQUID magnetic measurements.

Supporting Information Available: Detailed synthetic procedures and characterization methods, TEM and size histogram on more than 200 $Rh_{20}Fe_{80}$ NPs, EDX on an isolated $Rh_{20}Fe_{80}$ NP, XAS measurements at Rh and Fe K-edges and first derivative of the XANES part of the spectrum, EDX of the material after 1 h of reaction, and WAXS study as a function of time (PDF). This material is available free of charge via the Internet at http://pubs.acs.org.

CM0715343

(18) Margeat, O.; Dumestre, F.; Amiens, C.; Chaudret, B.; Lecante, P.; Respaud, M. *Prog. Solid State Chem.* **2005**, *33*, 71.
(19) Hayashi, K.; Sawada, M.; Harasawa, A.; Kimura, A.; Kakizaki, A. *Phys. Rev. B* **2001**, *64*, 054417-1.
(20) Ciuculescu, D.; Amiens, C.; Respaud, M.; Falqui, A.; Lecante, P.; Benfield, R. E.; Jiang, L.; Fauth, K.; Ballentine, G.; Friess, B.; Chaudret, B. Manuscript in preparation.
(21) Gatte, R. R.; Phillips, J. *J. Phys. Chem.* **1987**, *91*, 5961.
(22) Spisak, D.; Hafner, J. *Phys. Rev. B* **2006**, *73*, 155428.
(23) Pastor, G. M.; Dorantes-Davila, J.; Bennemann, K. H. *Phys. Rev. B* **1989**, *40*, 7642.
(24) Gruner, M. E.; Hoffmann, E.; Entel, P. *Phys. Rev. B* **2003**, *67*, 064415.